Hindawi
Journal of Nanomaterials
Volume 2019, Article ID 5154173, 5 pages
https://doi.org/10.1155/2019/5154173

Research Article

Molecular Simulations of Adsorption and Thermal Energy Storage of Mixed R1234ze/UIO-66 Nanoparticle Nanofluid

Qiang Wang,[1] Shengli Tang,[1] Sen Tian,[2] Xiaojian Wei,[3] and Tiefeng Peng[3]

[1]*Key Laboratory of Low-Grade Energy Utilization Technology & System, Ministry of Education, College of Energy and Power Engineering, Chongqing University, Chongqing 400044, China*
[2]*State Key Laboratory of Coal Mine Disaster Dynamics and Control, Chongqing University, Chongqing 400044, China*
[3]*Key Laboratory of Ministry of Education for Solid Waste Treatment and Resource Recycle, Southwest University of Science and Technology, Mianyang, Sichuan 621010, China*

Correspondence should be addressed to Sen Tian; sentian@cqu.edu.cn and Tiefeng Peng; pengtiefeng@cqu.edu.cn

Received 7 January 2019; Revised 24 May 2019; Accepted 30 May 2019; Published 16 June 2019

Academic Editor: Jean M. Greneche

In the process of adsorption and separation of fluid molecules on the solid surface of porous nanomaterials, the mutual transformation of thermal energy and surface energy can improve the heat absorption and energy utilization efficiency of circulating working medium. In this study, the adsorption, thermal energy storage, and mean square displacement of the minimum energy adsorption configuration of R1234ze in UIO-66 were studied by molecular simulations, including molecular dynamics (MD) and grand canonical Monte Carlo (GCMC) simulations. The results show that the thermal energy storage density of R1234ze/UIO-66 mixed working medium is significantly higher than that of pure working medium in the temperature range of 20 K-140 K. However, the increase rate of thermal energy storage density decreases significantly as temperature rises, and the mean square displacement and diffusion coefficient increase with increasing temperature.

1. Introduction

With the rapid development of modern society, serious problems, such as energy shortage and environmental pollution, have become increasingly prominent. Improving energy efficiency is one of the effective ways to maintain sustainable development [1, 2]. Thermal cycle is the main approach for energy conversion. Additionally, the working medium is the carrier of the thermodynamic cycle. Therefore, using various means to improve the thermal physical properties of the working medium can improve the energy conversion efficiency. Dispersing nanoparticles into traditional working fluids, e.g., water, alcohol, oil, and refrigerants, to produce uniform and stable nanofluids can effectively improve the heat transfer performance of the working medium [3–5]. Besides this, the unique energy storage mechanism of nanofluids is also developed by scientists.

Carbon nanotubes, zeolites, and metal-organic frameworks (MOFs) are common nanoporous materials, which have been applied in low cost and mass production in industry. These materials have a very large specific surface area compared to conventional materials. Thus, extra energy can be stored and output by the fluid desorbing/adsorbing in the nanoporous materials. Elsayed et al. [6, 7] studied the experimental characterization and energy storage feasibility of CPO-27 (Ni) MOF materials. The energy absorption of carbon nanotube nanofluids under thermal, mechanical, and electrical coupling fields was examined by Xu et al. and Chen et al. [8, 9], and several nanofluid systems have been designed. These systems have been proved to have a great potential for applications, including energy dissipation/absorption, energy capture, drive, and energy collection.

McGrail et al. [10] of the Northwest Pacific National Laboratory proposed that nanoscale MOFs should be added to the thermal cycle organic medium, and the new metal-organic heat carrier nanofluids (MOHCs) can be used to improve the efficiency of the thermodynamic cycle. MOHCs showed a great potential in low-grade energy utilization and

refrigeration cycles. MOFs are a class of organic-inorganic hybrid materials constructed from organic ligands and inorganic metal units. They own a large specific surface area, large porosity, diverse structures, and thermal stability, which have provided MOFs with a wide range of applications in the fields of energy, chemicals, materials, and so on [11, 12].

However, the nanopore structure in MOF is too small; it is difficult to study the adsorption and energy storage mechanism of organic materials in MOF by conventional experiments. Nowadays, with the rapid development of computational technology, modeling methods [13–15], e.g., molecular simulations [16–19], have been widely used in many fields. Its advantage is that it is not restricted by experimental conditions and can reveal the insights of macroscopical phenomena by studying the mechanism of material action.

Within various MOF structures, UIO-66 [20] is a metal-organic skeleton material containing Zr, which was developed by the University of Oslo in Norway in 2008. The material is made up of Zr's regular octahedron and 12 organic ligands to the two formic acid, forming a three-dimensional skeleton with a central hole cage with eight sides and eight tetrahedral cages. It is one of the most stable materials in metal-organic frameworks. Fluoroethane (R1234ze) [21] is an organic refrigerant commonly used in recent years. Its Ozone Depression Potential (ODP) is 0, and its Global Warming Potential (GWP) is less than 10. It has a good environmental friendly performance, thermal performance, and superior thermal storage property. Herein, R1234ze and UIO-66 were applied, and the adsorption, energy storage, and diffusion coefficient of R1234ze in UIO-66 were investigated to provide a theoretical basis for the application of R1234ze/UIO-66 nanofluids in the thermodynamic cycle.

2. Simulation Method

In theory, the endothermic energy (Δh_{MOHC}) of MOHC consists mainly of three parts [10, 22]: (a) phase transition enthalpy of organic medium ($\Delta h_{\mathrm{Fluid}}$), (b) internal energy change of MOF particles ($(\int C_p dT)_{\mathrm{MOF}}$), and (c) desorption energy of fluid medium in MOF. It can be expressed as follows, where x is the mass fraction of MOF in MOHC:

$$\Delta h\mathrm{MOHC} = \Delta h\mathrm{Fluid} + x \cdot \left(\left(\int Cpd\mathrm{T} \right) \mathrm{MOF} + \Delta h\mathrm{desorption} - \Delta h\mathrm{Fluid} \right). \quad (1)$$

At present, research on the thermophysical property of pure organic refrigerant is relatively mature, which can be obtained through experimental and theoretical methods. The National Institute of Standards and Technology (NIST) database [23] is widely employed in analyzing the thermophysical properties of pure fluid and thermodynamic cycles [1, 2]. Thus, the thermophysical data of R1234ze was retrieved via NIST. UIO-66 is a new type of material; the internal energy changes of the UIO-66 structure with temperature can be obtained by molecular dynamics (MD) simulations [24, 25]. The desorption heat of R1234ze in UIO-66 is calculated by grand canonical Monte Carlo (GCMC) simulations [26, 27].

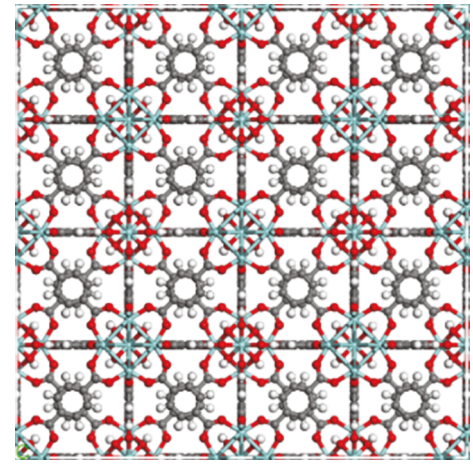

Figure 1: The calculation model of UIO-66 structure (2 × 2 × 2 unit cells of UIO-66).

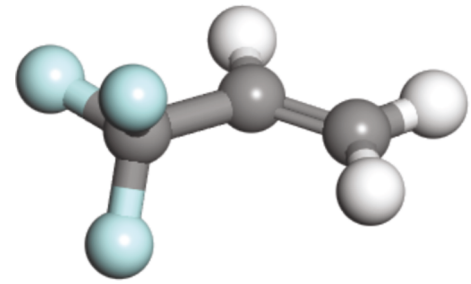

Figure 2: Molecular structure of organic refrigerant R1234ze (CH_2CHCF_3).

3. Simulation Processes

3.1. Structural Models. The computational model of the UIO-66 structure is composed of UIO-66 of 2 × 2 × 2 unit cells, as shown in Figure 1. Its size (Å) is X: 40.966, Y: 40.966, and Z: 40.966 and contains 3648 atoms (including 1536 C, 896 H, 1024 O, and 192 Zr). The molecular structure of R1234ze (CH_2CHCF_3) is shown in Figure 2.

The MD and GCMC simulations were performed by using Materials Studio [28]. The temperature of the system is controlled by the Berendsen method, and the periodic boundary conditions are applied to the X, Y, and Z directions of the simulation box. The COMPASS force field [29] was adopted to describe the intra- and intermolecular interactions. The Ewald summation method [30] is employed to correct the long-range Coulomb interactions.

3.2. UIO-66 Thermodynamics Energy. MD simulation is performed by the Forcite module in Materials Studio to calculate the internal energy change of UIO-66 particles at different temperatures in NVT ensemble. The time step is set to 1 fs. The temperatures were selected as 280 K, 300 K, 320 K, 340 K, 360 K, 380 K, 400 K, and 420 K. The system run for

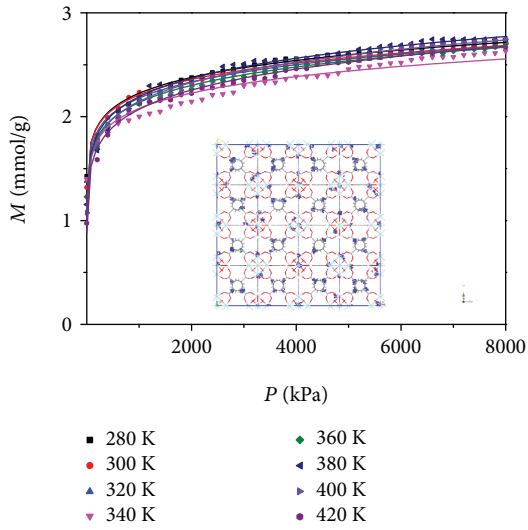

Figure 3: Adsorption isotherms snapshot of R1234ze in UIO-66.

1000 ps to reach the equilibration state. Then, the system run another 200 ps for statistics.

3.3. GCMC Simulated Adsorption Details. GCMC simulation selects the sorption module in Materials Studio to calculate the isothermal adsorption process of R1234ze at different temperatures in UIO-66. The simulated pressure range is set at 1-8000 kPa, corresponding to 280 K, 300 K, 320 K, 340 K, 360 K, 380 K, 400 K, and 420 K. The fugacity is calculated by the PR equation, and the simulation point is set to 40. The balance step of each calculation point is 400,000 cycles, and the statistical step is 500,000 cycles.

3.4. MSD Simulated Fluid Diffusion Details. In the sorption module of Materials Studio, the fixed pressure adsorption model is selected to calculate the minimum energy adsorption configuration under 280 K and 5000 kPa. The Forcite module in Materials Studio is selected to fix the porous material in the lowest energy configuration, and the kinetic simulation of the fluid molecule R1234ze in the minimum energy adsorption configuration is carried out in the NVT ensemble. The time step is set to 0.2 fs, and the analog continuous 40 ps. The calculated temperatures are 300 K, 320 K, 340 K, 360 K, 380 K, 400 K, and 420 K.

4. Results and Analysis

4.1. Isothermal Adsorption. The adsorption isotherms of R1234ze in UIO-66 are shown in Figure 3. The adsorption capacity of R1234ze in UIO-66 decreases as the temperature rises. In addition, because of the interaction between the fluid molecules and the UIO-66 solid surface, the R1234ze molecules are mainly adsorbed in the middle of the channels, and some of the R1234ze molecules are adsorbed around the skeleton. This indicates that the adsorption site of R1234ze in UIO-66 is selective.

4.2. Energy Storage Calculation. MD calculation can obtain the internal energy of UIO-66 in 280 K, 300 K, 320 K, 340 K, 360 K, 380 K, 400 K, and 420 K, as shown in Table 1. The

Table 1: The internal energy of UIO-66 at different temperatures via MD simulations.

Temperature (K)	Enthalpy (kcal/mol)
280	-195897.81
300	-194924.48
320	-194010.51
340	-193369.76
360	-193051.10
380	-192269.17
400	-192359.21
420	-191762.94

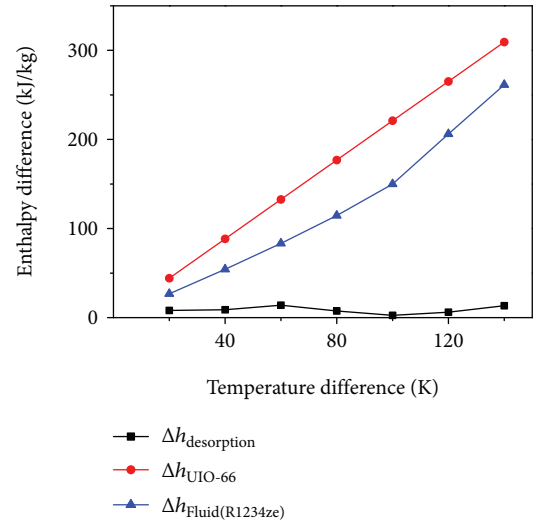

Figure 4: Relationship between specific enthalpy difference and temperature difference of 280 K-420 K under 5 MPa.

internal energy value of UIO-66 particles increases as the temperature rises, which is in line with the general law of the temperature change of solid materials. The specific heat capacity of UIO-66 is $Cp = 2.21$ (kJ/kg K) by corresponding calculation. This is different from the data reported [26, 31, 32] in the literature, mainly due to the different structures and components of MOFs.

According to formula (1), the specific enthalpy difference $\Delta h_{\text{UIO-66}}$ and desorption heat $\Delta h_{\text{desorption}}$ of UIO-66 in mixed working medium R1234ze/UIO-66 are calculated. The 280 K-420 K specific enthalpy value of R1234ze under 5 MPa can be found through NIST, and the relationship between the specific enthalpy difference Δh_{Fluid} and the temperature difference can be calculated, as shown in Figure 4. This study takes 5 MPa as the reference pressure. The relationship between the increase rate of the energy storage density of the R1234ze/UIO-66 mixture with different mass fraction of UIO-66 particles in the heat absorption process with the temperature difference of the cold source (280 K) is shown in Figure 5.

The analysis of Figure 5 can draw a conclusion that using 280 K as a cold and heat source and within the temperature difference of 140 K, adding UIO-66 particles to the organic medium R1234ze helps to improve the thermal energy

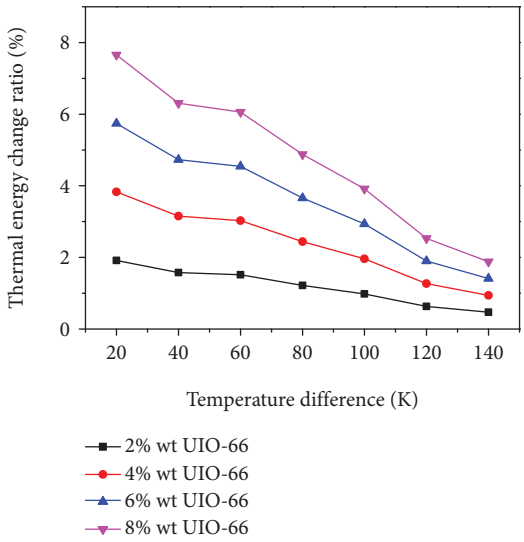

Figure 5: Relationship between 280 K-420 K energy storage rate and temperature difference of R1234ze/UIO-66 mixed working medium under 5 MPa.

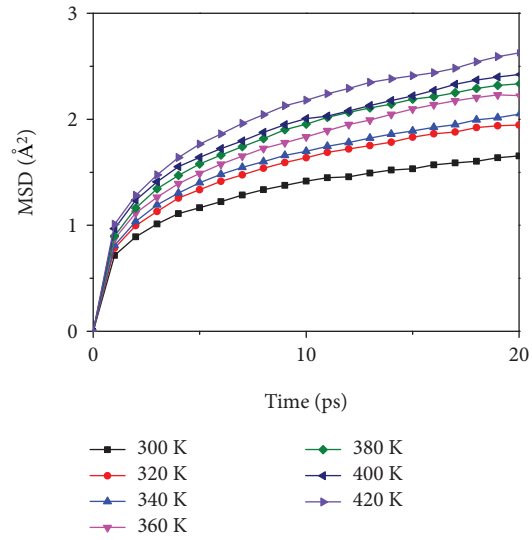

Figure 6: Mean square displacement of 280 K and 5000 kPa adsorption configurations at different temperatures.

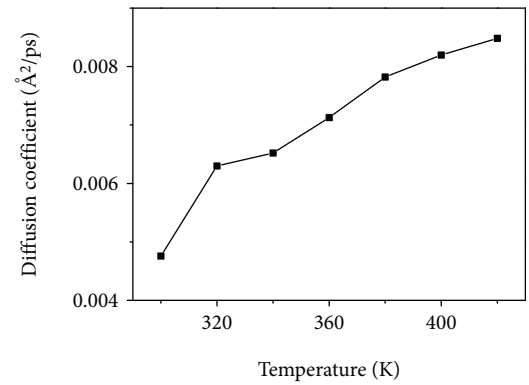

Figure 7: The diffusion coefficient of 280 K and 5000 kPa lowest energy adsorption configuration at different temperatures.

storage density of R1234ze, and the density of thermal energy storage increases as the UIO-66 mass fraction rises. However, with the increase of temperature difference, the increase rate of energy storage density is obviously reduced. The analysis of Figure 4 shows that this is due to the reduction of the desorption of heat in the mixture of medium material as the temperature rises. At the same time, from Figure 4, it can be found that as the $\Delta h_{\text{UIO-66}}$ is higher than $\Delta h_{\text{Fluid(R1234ze)}}$ under all temperature differences, the density phase of the mixture can be improved in all working conditions.

4.3. MSD and Diffusion Coefficient. In order to study the kinetic characteristics of adsorbed molecule R1234ze at different temperatures, a saturated adsorption model was developed. Here, the kinetic simulation of the R1234ze molecules in the adsorption configuration under 280 K and 5000 kPa is carried out, and the mean square displacement and diffusion coefficient at different temperatures are analyzed, as shown in Figures 6 and 7. The analysis of Figure 6 shows that the mean square displacement (MSD) at the same temperature increases linearly with time. Meanwhile, the mean square displacement increases as the temperature rises. The diffusion coefficient characterizes the motion ability of the fluid molecule R1234ze at different temperatures. Figure 7 shows that the diffusion coefficient increases as the temperature rises.

5. Conclusions

The adsorption, thermal energy storage, and diffusion coefficient of R1234ze in UIO-66 were studied by MD and GCMC simulation methods. The thermal energy storage density of R1234ze/UIO-66 under different working conditions was predicted by comparison with the theoretical model. The following observations and conclusions can be drawn: (1) adding UIO-66 particles in organic R1234ze can enhance the thermal energy storage density of R1234ze, and the thermal energy storage density increases as the UIO-66 mass fraction rises; (2) however, the increase rate of thermal energy storage density decreases as the temperature rises; (3) under the working condition of this study, the mean square displacement increases as the temperature rises, and the diffusion coefficient increases as the temperature rises.

Data Availability

The data used to support the findings of this study are available from the corresponding author upon request.

Conflicts of Interest

The authors declare no conflict of interest.

Acknowledgments

This work is supported by the National Natural Science Foundation of China (Nos. 51506013, 51704047), Chongqing

Research Program of Basic Research and Frontier Technology (No. cstc2018jcyjAX0522), and Doctoral Foundation of Southwest University of Science and Technology (Nos. 17zx7161 and 17LZXT05).

References

[1] C. Zhang, C. Liu, S. Wang, X. Xu, and Q. Li, "Thermo-economic comparison of subcritical organic Rankine cycle based on different heat exchanger configurations," *Energy*, vol. 123, pp. 728–741, 2017.

[2] S. Wang, C. Liu, C. Zhang, X. Xu, and Q. Li, "Thermo-economic evaluations of dual pressure organic Rankine cycle (DPORC) driven by geothermal heat source," *Journal of Renewable and Sustainable Energy*, vol. 10, no. 6, article 063901, 2018.

[3] S. U. S. Choi, Z. G. Zhang, W. Yu, F. E. Lockwood, and E. A. Grulke, "Anomalous thermal conductivity enhancement in nanotube suspensions," *Applied Physics Letters*, vol. 79, no. 14, pp. 2252–2254, 2001.

[4] R. Saidur, K. Y. Leong, and H. A. Mohammad, "A review on applications and challenges of nanofluids," *Renewable and Sustainable Energy Reviews*, vol. 15, no. 3, pp. 1646–1668, 2011.

[5] Q. Li and C. Liu, "Molecular dynamics simulation of heat transfer with effects of fluid–lattice interactions," *International Journal of Heat and Mass Transfer*, vol. 55, no. 25-26, pp. 8088–8092, 2012.

[6] A. Elsayed, E. Elsayed, R. Al-Dadah, S. Mahmoud, A. Elshaer, and W. Kaialy, "Thermal energy storage using metal–organic framework materials," *Applied Energy*, vol. 186, pp. 509–519, 2017.

[7] E. Elsayed, R. Al-Dadah, S. Mahmoud, P. A. Anderson, A. Elsayed, and P. G. Youssef, "CPO-27(Ni), aluminium fumarate and MIL-101(Cr) MOF materials for adsorption water desalination," *Desalination*, vol. 406, pp. 25–36, 2017.

[8] B. Xu, L. Liu, H. Lim, Y. Qiao, and X. Chen, "Harvesting energy from low-grade heat based on nanofluids," *Nano Energy*, vol. 1, no. 6, pp. 805–811, 2012.

[9] X. Chen, B. Xu, and L. Liu, "Nanoscale fluid mechanics and energy conversion," *Applied Mechanics Reviews*, vol. 66, no. 5, pp. 050803–050803, 2014.

[10] B. P. McGrail, P. K. Thallapally, J. Blanchard, S. K. Nune, J. J. Jenks, and L. X. Dang, "Metal-organic heat carrier nanofluids," *Nano Energy*, vol. 2, no. 5, pp. 845–855, 2013.

[11] H. Furukawa, K. E. Cordova, M. O'Keeffe, and O. M. Yaghi, "The chemistry and applications of metal-organic frameworks," *Science*, vol. 341, no. 6149, article 1230444, 2013.

[12] S. L. James, "Metal-organic frameworks," *Chemical Society Reviews*, vol. 32, no. 5, pp. 276–288, 2003.

[13] H. Zhang, C. Liu, X. Xu, and Q. Li, "Mechanism of thermal decomposition of HFO-1234yf by DFT study," *International Journal of Refrigeration*, vol. 74, pp. 399–411, 2017.

[14] G. Lei, C. Liu, Q. Li, and X. Xu, "Graphyne nanostructure as a potential adsorbent for separation of H_2S/CH_4 mixture: combining grand canonical Monte Carlo simulations with ideal adsorbed solution theory," *Fuel*, vol. 182, pp. 210–219, 2016.

[15] M. Wang, C. Liu, X. Xu, and Q. Li, "Theoretical investigation on the carbon sources and orientations of the aldehyde group of furfural in the pyrolysis of glucose," *Journal of Analytical and Applied Pyrolysis*, vol. 120, pp. 464–473, 2016.

[16] Q. Li, C. Liu, and X. Chen, "Molecular dynamics simulation of sulphur nucleation in S–H_2S system," *Molecular Physics*, vol. 112, no. 7, pp. 947–955, 2014.

[17] Q. Li, C. Liu, and Z. Zhang, "Prediction of solubility of sulfur in hydrogen sulfide based on molecular dynamics simulation," *Asian Journal of Chemistry*, vol. 26, no. 4, pp. 1041–1043, 2014.

[18] X. Shi, Q. Li, T. Wang, and K. S. Lackner, "Kinetic analysis of an anion exchange absorbent for CO_2 capture from ambient air," *PLoS One*, vol. 12, no. 6, article e0179828, 2017.

[19] C. Huang, X. Peng, B. Yang et al., "Anisotropy effects in diamond under nanoindentation," *Carbon*, vol. 132, pp. 606–615, 2018.

[20] M. J. Katz, Z. J. Brown, Y. J. Colon et al., "A facile synthesis of UiO-66, UiO-67 and their derivatives," *Chemical Communications*, vol. 49, no. 82, pp. 9449–9451, 2013.

[21] A. Yataganbaba, A. Kilicarslan, and İ. Kurtbaş, "Exergy analysis of R1234yf and R1234ze as R134a replacements in a two evaporator vapour compression refrigeration system," *International Journal of Refrigeration*, vol. 60, pp. 26–37, 2015.

[22] Q. Li, Y. Xiao, X. Shi, and S. Song, "Rapid evaporation of water on graphene/graphene-oxide: a molecular dynamics study," *Nanomaterials*, vol. 7, no. 9, p. 265, 2017.

[23] NISThttp://webbook.nist.gov/chemistry/fluid/.

[24] Q. Li, M. Wang, Y. Liang et al., "Molecular dynamics simulations of aggregation of copper nanoparticles with different heating rates," *Physica E: Low-dimensional Systems and Nanostructures*, vol. 90, pp. 137–142, 2017.

[25] Q. Li, Y. Yu, Y. Liu, C. Liu, and L. Lin, "Thermal properties of the mixed n-octadecane/Cu nanoparticle nanofluids during phase transition: a molecular dynamics study," *Materials*, vol. 10, no. 1, p. 38, 2017.

[26] J. Hu, C. Liu, Q. Li, and X. Shi, "Molecular simulation of thermal energy storage of mixed CO_2/IRMOF-1 nanoparticle nanofluid," *International Journal of Heat and Mass Transfer*, vol. 125, pp. 1345–1348, 2018.

[27] J. Hu, C. Liu, L. Liu, and Q. Li, "Thermal energy storage of R1234yf, R1234ze, R134a and R32/MOF-74 nanofluids: a molecular simulation study," *Materials*, vol. 11, no. 7, p. 1164, 2018.

[28] I. Accelrys, *Materials Studio*, Accelrys Software Inc, 2010.

[29] H. Sun, "COMPASS: an ab initio force-field optimized for condensed-phase applications overview with details on alkane and benzene compounds," *The Journal of Physical Chemistry B*, vol. 102, no. 38, pp. 7338–7364, 1998.

[30] I.-C. Yeh and M. L. Berkowitz, "Ewald summation for systems with slab geometry," *The Journal of Chemical Physics*, vol. 111, no. 7, pp. 3155–3162, 1999.

[31] Q. Wang, S. Tang, and L. Li, "Energy storage analysis of a mixed R161/MOF-5 nanoparticle nanofluid based on molecular simulations," *Materials*, vol. 11, no. 5, p. 848, 2018.

[32] B. Mu and K. S. Walton, "Thermal analysis and heat capacity study of metal–organic frameworks," *The Journal of Physical Chemistry C*, vol. 115, no. 46, pp. 22748–22754, 2011.